Available online at www.sciencedirect.com
SCIENCE DIRECT
Biochemical Pharmacology 69 (2005) 913–927
Biochemical Pharmacology
www.elsevier.com/locate/biochempharm

Mitochondrial-dependent, reactive oxygen species-independent apoptosis by myricetin: roles of protein kinase C, cytochrome c, and caspase cascade

Ching Huai Ko [a], Shing-Chuan Shen [b,c], Chun-Sen Hsu [d], Yen-Chou Chen [e,*]

[a] *Graduate Institute of Pharmacy, School of Pharmacy, Taipei Medical University, Taipei, Taiwan*
[b] *Department of Dermatology, School of Medicine, Taipei Medical University, Taipei, Taiwan*
[c] *Department of Dermatology, Taipei Municipal Wan-Fang Hospital, Taipei, Taiwan*
[d] *Department of Obstetrics and Gynecology Taipei Municipal Wan-Fang Hospital-Affiliated Taipei Medical University, Taipei, Taiwan*
[e] *Graduate Institute of Pharmacognosy, School of Pharmacy, Taipei Medical University, Taipei, Taiwan*

Received 24 September 2004; accepted 6 December 2004

Abstract

Abrogation of mitochondrial permeability and induction of reactive oxygen species (ROS) production have been observed in chemical-induced apoptosis; however, the relationship between the mitochondria and intracellular ROS levels in apoptosis is still unclear. In the present study, myricetin (ME) but not its respective glycoside, myricitrin (MI; myricetin-3-*O*-rhamnose) reduced the viability of human leukemia HL-60 cells via apoptosis, characterized by the occurrence of DNA ladders and hypodiploid cells. Results of Western blotting and caspase activity assays showed that activation of caspases 3 and 9 but not caspases 1, 6 or 8 with cleavage of PARP and D4-GDI proteins is involved in ME-induced apoptosis. A reduction in mitochondrial functions characterized by a decrease in the Bcl-2/Bax protein ratio and translocation of cytochrome c (cyt c) from the mitochondria to the cytosol in accordance with a decrease in mitochondrial membrane potential were observed in ME-treated HL-60 cells. No significant induction of intracellular ROS levels by ME was observed by the DCHF-DA assay, DPPH assay or plasmid digestion assay, and antioxidants including *N*-acetyl-cysteine (NAC), catalase (CAT), superoxide dismutase (SOD), and tiron (TIR) showed no protective effects on ME-induced apoptosis. A PKC activator, 12-*O*-tetradecaoylphorbol-13-acetate (TPA) significantly attenuated ME-induced apoptosis via preventing cytochrome c release to the cytosol and maintaining the mitochondrial membrane potential by inhibiting the decrease in the Bcl-2/Bax protein ratio; these effects were blocked by protein kinase C (PKC) inhibitors including GF-109203X, H7, and staurosporin. Removing mitochondria by ethidium bromide (EtBr) treatment reduced the apoptotic effect of ME. Results of SAR studies showed that the presence of OH at C3′, C4′, and C5′ is important for the apoptosis-inducing activities of ME, and that ME induces apoptosis in another leukemia cell line, Jurkat cells, but not in primary human polymorphonuclear (PMN) cells or in murine peritoneal macrophages (PMs). The results of the present study suggest that apoptosis induced by ME occurs through a novel mitochondrion-dependent, ROS-independent pathway; TPA protects cells from ME-induced apoptosis via PKC activation which prevents the occurrence of mitochondrial destruction during apoptosis.

Keywords: Myricetin; Mitochondria; Reactive oxygen species; TPA; Cytochrome c

1. Introduction

Mitochondria plays central role in cellular metabolism and apoptosis. During apoptosis, a wide variety of cellular signals elicited from the membrane, cytosol or mitochondria are activated by stimuli. These signals can disturb redox and energy metabolism and modulate the expression of Bcl-2 family members [1]. Mitochondria may sense the death signals and commit cells to apoptosis by releasing

Abbreviations: BCIP, 5-bromo-4-chloro-3-indolyl-phosphate; Bcl-2, B-cell lymphoma-2; CAT, catalase; cyt c, cytochrome c; DCHF-DA, dichlorodihydrofluorescein diacetate; GF, GF-109203X; H-7, isoquinoline-5-sulfonic 2-methyl-1-piperazide; ME, myricetin; MI, myricitrin; NAC, *N*-acetyl-cysteine; NBT, nitro blue tetrazolium; PKC, protein kinase C; PMN cells, polymorphonuclear cells; PMs, murine peritoneal macrophages; ROS, reactive oxygen species; SOD, superoxide dismutase; ST, staurosporine; TIR, tiron; TPA, 12-*O*-Tetradecaoylphorbol-13-acetate

* Corresponding author. Tel.: +886 2 27361661x6152; fax: +886 2 23787139.
E-mail address: yc3270@tmu.edu.tw (Y.-C. Chen).

0006-2952/$ – see front matter © 2004 Elsevier Inc. All rights reserved.
doi:10.1016/j.bcp.2004.12.005

death factors into the cytosol, such as cytochrome c (cyt c). Cyt c plays roles in triggering apoptosis and maintaining the oxidative phosphorylation of mitochondria, and the cyt c released into the cytosol binds to Apaf-1 to form a complex with caspase 9, followed by activation of downstream caspases to cleave cellular substrates [2,3].

Mitochondria are a major source of intracellular reactive oxygen species (ROS) production, and ROS have been implicated as second messengers and are known to participate in physiological processes, such as apoptosis and proliferation. Previous studies reported that proliferation induced by epidermal growth factor (EGF) or platelet-derived growth factor (PDGF) was mediated by ROS production and ROS have been shown to induce proliferation in tumor progression [4,5]. Therefore, antioxidants possess an effective inhibitory effect on the promotion of tumors via reducing ROS production. In addition, ROS have been suggested to induce apoptosis and apoptosis induced by anticancer drugs such as taxol and etoposide is mediated by an increase in intracellular ROS production [6,7]. These data indicate correlations among ROS, mitochondria, and apoptosis, however, whether cross-talk exists between ROS and mitochondria is still unclear.

Anti-apoptotic Bcl-2 family proteins such as Bcl-2 and Bcl-XL are proto-oncoproteins and prevent the morphological changes of apoptosis induced by death stimuli. It has been suggested that the anti-apoptotic effect of Bcl-2 might occur through regulating the cellular redox potential via increasing the GSH pool or redistributing GSH to the mitochondria and thus, preventing ROS production and cellular damage caused by oxidative stresses [8]. However, Steinman suggested a pro-oxidant effect for Bcl-2 [9]. Previous studies showed that anti-apoptotic Bcl-2 family proteins such as Bcl-2 and Bcl-XL prevent the occurrence of apoptosis via regulating mitochondrial homeostasis and blocking cyt c release and caspase activation [10]. In addition to anti-apoptotic Bcl-2 family proteins, the oligomerization of apoptotic Bcl-2 family proteins such as Bax forms mitochondrial transmembrane channels and triggers the release of apoptotic factors into the cytoplasm thus, initiating a mitochondrion-dependent pathway of apoptosis execution [11]. However, the mechanism of Bcl-2 family proteins in regulating ROS production and mitochondrial functions during apoptosis is still undefined.

12-*O*-Tetradecanoylphorbol 13-acetate (TPA) has been used as a potent tumor promoter in mouse skin models, and protein kinase C (PKC) is one of the early genes activated by TPA. Activation of PKC by TPA is mediated by translocation of PKC protein from the cytosol to the membrane and transduction of signals into cells [12]. Bezombes et al. showed that activation of protein kinase C was able to inhibit apoptosis induced by ROS via blocking caspase activation [13]. Harper et al. demonstrated that PKC activation inhibited trail-induced apoptosis and TNF-induced NF-kB activation [14]. However, PKC-dependent apoptosis was elucidated in previous studies [15,16]. These data suggest that activation of PKC might block or promote the progression of apoptosis; however, the effect of PKC in regulating mitochondrial homeostasis during apoptosis is still unclear.

Recently, we reported the antitumor and anti-inflammatory mechanisms of flavonoids in vitro and in vivo [17,18]. We found that flavonoids possess the ability to reduce the viability of tumor cells via inducing apoptosis, and that both ROS-dependent and -independent pathways are involved [19,20]. This study further addresses the roles of ROS production, release of cyt c from mitochondria to the cytoplasm, caspase activation, and mitochondrial functions in cell death induced by the flavonoid, myricetin (ME). We show that mitochondrion-dependent and ROS-independent apoptosis is induced by ME, and PKC activation induced by TPA negatively regulates the occurrence of apoptosis via the maintenance of mitochondrial homeostasis.

2. Materials and methods

2.1. Cell culture

HL-60 human promyeloleukemic cells and THP-1 mature monocytic cells were obtained from ATCC (American Type Culture Collection; Rockville, MD). The mouse primary cultured macrophages (PM) were obtained as described in a previous study [15]. Human polymorphonuclear (PMN) cells were obtained from healthy male donors after Ficoll-Hypaque density gradient separation. Human PMN cells were washed twice in 0.9% NaCl and resuspended in RPMI1640 medium. HL-60 and THP-1 cells were grown in RPMI1640 containing 10% heat-inactivated fetal bovine serum (FBS) and maintained at 37 °C in a humidified incubator containing 5% CO_2. Exponentially growing cells were exposed to drugs for the indicated time periods. All cultural reagents were purchased form Gibco/BRL.

2.2. Chemicals

The colorigenic synthetic peptide substrates, Ac-DEVD-pNA, Ac-YVAD-pNA, Ac-IETD-pNA, and Ac-LEHD-pNA, as well as the protease inhibitors for Ac-DEVD-FMK, Ac-YVAD-FMK, Ac-IETD-FMK, and Ac-LEHD-FMK were purchased from Calbiochem. 12-*O*-Tetradecanoylphorbol 13-acetate, propidium iodide, staurosporine, H-7 (isoquinoline-5-sulfonic 2-methyl-1-piperazide), and 3-(4,5-dimethylthiazol-2-yl)-2,5-diphenyl tetrazolium bromide (MTT) were obtained from Sigma (St. Louis, MO, USA). GF-109203X was purchased from Calbiochem. Myricetin, myricitrin (MI), flavone, galangin, myricetin-trimethylether, ethidium bromide, and other chemicals were purchased from Sigma. Antibodies for PARP, caspase 3, and D4-GDI detection in Western blotting were obtained from

IMGENEX. Antibodies for detecting Bcl-2 family proteins and α-tubulin were purchased from Santa Cruz. Dichlorodihydrofluorescein diacetate (DCHF-DA) and DiOC6(3) were obtained from molecular probe.

2.3. Cell viability

Cell viability was assessed by MTT staining as described previously [21]. Briefly, HL-60 cells were plated at a density of 10^5 cells/well into 24-well plates. After overnight growth, cells were treated with a different concentration of flavonoids described above for 12 h. At the end of treatment, 30 μl of the tetrazolium compound, MTT, and 270 μl of fresh RPMI medium were added. The supernatant was removed and formazan crystals were dissolved by DMSO. After incubation for 4 h at 37 °C, 200 μl of 0.1 N HCl in 2-propanol was placed in each well to dissolve the tetrazolium crystals. Finally, the absorbance at a wavelength of 600 nm was recorded using an ELISA plate reader.

2.4. Determination of ROS production

ROS production was monitored by flow cytometry using DCHF-DA [22]. This dye is a stable compound that readily diffuses into cells and is hydrolyzed by intracellular esterase to yield DCHF, which is trapped within cells. Hydrogen peroxide or low-molecular weight peroxides produced by cells oxidize DCHF to the highly fluorescent compound, 2′,7′-dichlorofluorescein (DCF). Thus, the fluorescence intensity is proportional to the amount of peroxide produced by the cells. In the present study, HL-60 cells were treated with each indicated flavanone (40 μM) for 2 or 4 h, respectively. Then, indicated flavanone-treated cells were washed twice with PBS to remove the extracellular compounds and DCHF-DA (100 μM) with or without H_2O_2 (200 μM) was added for an additional hour. Green fluorescence was excited using an argon laser and was detected using a 525-nm band-pass filter by flow cytometric analysis.

2.5. Western blots

Total cellular extracts (20 μg) were prepared and separated on 8% SDS–polyacrylamide mini gels for PARP detection and 12% SDS–polyacrylamide minigels for caspase 3, cleaved D4-GDI, the Bcl-2 family, and α-tubulin detection, and transferred to immobilon polyvinylidene difluoride membranes (Millipore). The membranes were incubated at 4 °C with 1% bovine serum albumin at room temperature for 1 h and then incubated with the indicated antibodies for a further 3 h at room temperature followed by incubation with alkaline phosphatase-conjugated anti-mouse IgG antibody for 1 h. Protein was visualized by incubating with the colorimetric substrates, nitro blue tetrazolium (NBT) and 5-bromo-4-chloro-3-indolyl-phosphate (BCIP), as described in our previous papers [18–20].

2.6. Release of cytochrome c from mitochondria in drug-treated cells

Untreated and drug-treated cells were harvested by centrifugation at 1000 × *g* for 5 min at 4 °C. Cell pellets were washed once with ice-cold PBS and resuspended with 5 volumes of 20 mM HEPES-KOH (pH 7.5), 10 mM KCl, 1.5 mM $MgCl_2$, 1 mM EDTA, 1 mM EGTA, 1 mM DTT, 0.1 mM PMSF, and 250 mM sucrose. Cells were homogenized and centrifuged at 750 × *g* for 10 min at 4 °C. Supernatants were then centrifuged at 10,000 × *g* for 15 min at 4 °C. Pellets were lysed with 0.1 ml of lysis buffer consisting of 10 mM Tris–HCl (pH 7.4), 1 mM EDTA, 1 mM EGTA, 0.15 M NaCl, 5 μg/ml aprotinin, 5 μg/ml leupeptin, 0.5 mM PMSF, 2 mM sodium orthovanadate, and 1% SDS. The lysed solution was used for the identification of mitochondrial cytochrome c by immunoblotting. The supernatants were centrifuged at 100,000 × *g* for 15 min at 4 °C and the obtained supernatants were used for identification of cytosolic cytochrome c by immunoblotting.

2.7. DNA gel electrophoresis

Cells (10^6/ml) under different treatments were collected, washed with PBS twice, then lysed in 100 ml of lysis buffer (50 mM Tris, pH 8.0; 10 mM ethylenediaminetetraacetic acid (EDTA); 0.5% sodium sarkosinate, and 1 mg/ml proteinase K) for 3 h at 56 °C and treated with 0.5 mg/ml RNase A for another hour at 56 °C. DNA was extracted with phenol/chloroform/isoamyl alcohol (25/24/1) before loading. Samples were mixed with loading buffer (50 mM Tris, 10 mM EDTA, 1% (w/w) low-melting-point agarose, 0.025% (w/w) bromophenol blue) and loaded onto a pre-solidified 2% agarose gel containing 0.1 μg/ml ethidium bromide. The agarose gels were run at 50 V for 90 min in TBE buffer, then observed and photographed under UV light.

2.8. Assay of alkaline phosphatase activity

The activity of alkaline phosphatase was determined as Field et al. reported [23]. Briefly, 8.44 mM *p*-nitrophenyl phosphate was used as the substrate in 0.2 M glycine buffer (pH 9.8), containing 0.5 mM $MgCl_2$ and 1.6 μM zinc chloride. Aliquots containing 50 μg of protein in 50 μl of Tris buffer (pH 7.4) were incubated with 200 μl of the substrate solution at 37 °C for 30 min. The incubation mixture was then centrifuged at 13,000 × *g* for 5 min and the absorbance of the supernatant was measured at 405 nm to determine the amount of *p*-nitrophenol released by the enzyme.

2.9. Ethidium bromide treatment of cultured cells

Mitochondria-depleted HL 60 cells (p^0 cells) were generated by propagating HL 60 cells (p^+ cells) in the

presence of 50 ng/ml EtBr (Sigma) for 4 weeks as Larm et al. reported [24–26]. During this period and for subsequent propagation of EtBr-treated cells, the growth medium was further supplemented with 1 mM pyruvate and 50 pg/ml uridine. Cultures were sampled at weekly intervals and assayed for whole-cell NADH-ferricyanide reductase activity, cyanide-sensitive oxygen uptake, and the presence of mtDNA.

2.10. Measurement of the mitochondrial membrane potential

After ME treatments, HL-60 cells were incubated with 40 nM DiOC6(3) for 15 min at 37 °C. Then, cells were washed with ice-cold PBS and collected by centrifugation at 500 × *g* for 10 min. The collected cells were then resuspended in 500 μl of PBS containing 40 nM DiOC6(3). Fluorescence intensities of DiOC6(3) were analyzed on a flow cytometer (FACScan, Becton Dickinson, San Jose, CA) with excitation and emission settings of 484 and 500 nm, respectively.

2.11. Analysis of respective caspase activities

Ac-DEVD-pNA for caspase 3, Ac-YVAD-pNA for caspase 1, Ac-IETD-pNA for caspase 8, and Ac-LEHD-pNA for caspase 9 were used as colorimetric protease substrates. After different treatments, cells were collected and washed three times with PBS and resuspended in 50 mM Tris–HCl (pH 7.4), 1 mM EDTA, and 10 mM ethyleneglycoltetraacetic acid (EGTA). Cell lysates were clarified by centrifugation at 15,000 rpm for 3 min, and clear lysates containing 50 μg of protein were incubated with 100 μM of the indicated specific colorimetric substrates at 37 °C for 1 h. Alternative activities of caspases 1, 3, 8, and 9 enzymes were described as the cleavage of colorimetric substrate by measuring the absorbance at 405 nm.

2.12. DPPH radical-scavenging activity assay

The scavenging activities of compounds against DPPH radicals were measured according to a previous study [27]. In brief, different concentrations of compounds were added to 0.1 ml of 1 M Tris–HCl buffer (pH 7.9) and then mixed with 1.2 ml of 500 mM DPPH in methanol for 20 min while being protected from light. The absorbance at 517 nm was determined. Deionized water was used as a control group. The decrease of absorbance at 517 nm was used to calculate the scavenging activity.

2.13. Flow cytometric analysis

Trypsinized cells were washed with ice-cold PBS and fixed in 70% ethanol at −20 °C for at least 1 h. After fixation, cells were washed twice, incubated in 0.5 ml of 0.5% Triton X-100/PBS at 37 °C for 30 min with 1 mg/ml of RNase A, and stained with 0.5 ml of 50 mg/ml propidium iodide for 10 min. The fluorescence emitted from the propidium–DNA complex was quantitated after excitation of the fluorescent dye by FACScan flow cytometry (Becton Dickenson).

2.14. Plasmid digestion assay

Covalently closed circular plasmid pBR322 DNA (0.25 μg) in a final volume of 30 μl was treated with varying concentrations of tetracycline (0.1–2.0 mM) in the presence and absence of Cu(II) ions and exposed to white light for 2 h. To this, 6 μl of 5× tracking dye (40 mM EDTA, 0.05% bromophenol blue, and 50 vol.% glycerol) was added and loaded onto 0.8% agarose gels. The gel was run at 50 mA and stained with ethidium bromide (0.5 μg/ml), for 30 min at 4 °C. After washing, the bands were visualized on a UV-transilluminator and photographed [28].

2.15. Statistical analysis

Values are expressed as the mean ± S.E. The significance of the difference from the respective controls for each experimental test condition was assayed using Student's *t*-test for each paired experiment. A *p*-value of <0.01 or <0.05 was regarded as indicating a significant difference.

3. Results

3.1. Myricetin exhibits significant cytotoxicity in HL-60 human leukemia cells

Myricetin exists extensively in plants including fruits, vegetables, and various Chinese herbs. However, the apoptotic effect of myricetin is still unclear. As illustrated in Fig. 1A, myricetin and its glycoside, myricitrin, share the same main structure except for a rhamnoside at C3 of MI. Results of the MTT assay showed that ME but not MI exhibited dose- and time-dependent cytotoxicity in HL-60 cells, and the IC_{50} of ME was 42.25 μM (Fig. 1A). In order to identify, if ME-induced cell death occurs via apoptosis, the apoptotic characteristics including DNA integrity, apoptotic bodies, and hypodiploid cells in ME-treated cells were examined. Results in Fig. 1B show that ME but not MI dose-dependent and time-dependent induce the occurrence of DNA ladders in cells. Appearance of apoptotic bodies was examined in ME (but not MI)-treated cells under microscopic observations (Fig. 1C) and an increase in the ratio of hypodiploid cells (sub-G1 peak) was found in ME- but not MI-treated HL-60 cells (Fig. 1D and E). These data suggest that ME but not its glycoside, MI, possesses the ability to reduce the viability of HL-60 leukemia cells via apoptosis induction.

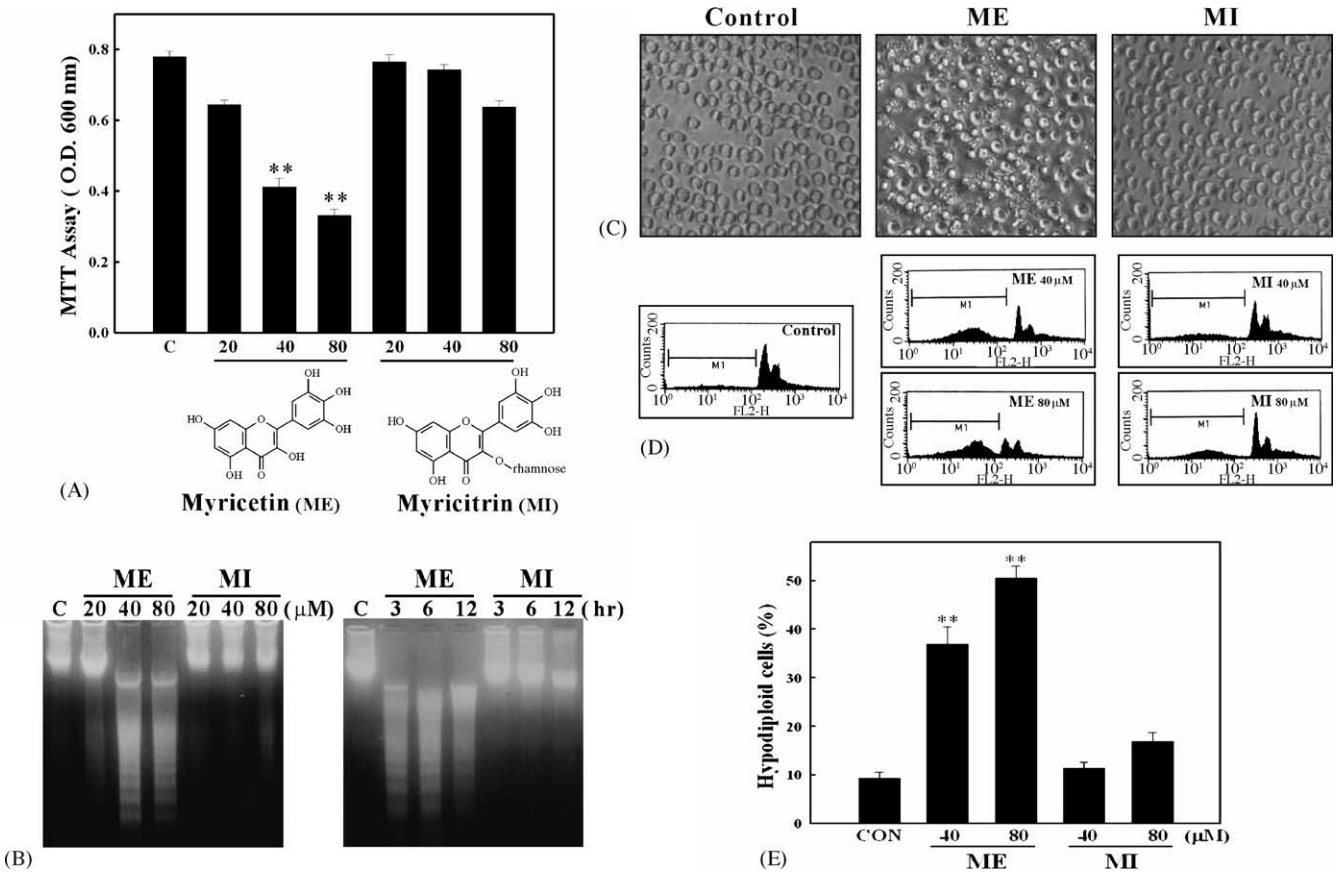

Fig. 1. Myricetin but not myricitrin exhibited an apoptotic effect in human HL-60 leukemia cells. (A) HL-60 cells were treated with different concentrations of myricetin and myricitrin (20, 40, and 80 μM) for 12 h. MTT was added to the medium for a further 4 h. The viability of cells was detected by measuring the absorbance at a wavelength of 600 nm. Each value is presented as the mean ± S.E. of three independent experiments. (**) $p < 0.01$ significantly different from the control group as analyzed by Student's *t*-test. The chemical structures of ME and MI are described below the data. (B) (Right panel) HL-60 cells were treated with different concentrations (20, 40, and 80 μM) of ME and MI for 12 h, and DNA from cells was extracted and electrophoresed through a 1.8% agarose gel and visualized by staining with ethidium bromide. (Left panel) similarly, HL-60 cells were treated with ME or MI (80 μM) for different time points (3, 6, and 12 h) and the appearance of DNA ladders was detected. (C) ME but not MI induced apoptotic bodies in HL-60 cells. Cells were treated with ME or MI (80 μM) and the morphology of cells was observed microscopically. (D) ME but not MI induced hypodiploid cells in HL-60 cells. Cells were treated with ME or MI (40 and 80 μM) and hypodiploid cells were examined by flow cytometric analysis. A representative of three experiments is presented here. (E) Quantification of the results derived from (D) was performed. Each value is presented as the mean ± S.E. of three independent experiments. (**) $p < 0.01$ significantly different from the control as analyzed by Student's *t*-test.

3.2. Activation of caspases 3 and 9 but not caspases 1, 6, and 8 enzymes is involved in ME-induced apoptosis

Activation of caspase cascades has been shown to occur in apoptosis; however, the types of caspases activated in ME-induced apoptosis are still undefined. Results of Western blotting showed that ME but not its glycoside, MI, induced the cleavage of caspase 3 protein with degradation of the caspase 3 substrate proteins, PARP and D4-GDI (Fig. 2A). A decrease in Bcl-2 protein and an increase in Bax and Bad proteins were detected in dose-dependent manners with ME treatment. Results of quantification of Bcl-2 and Bax protein intensities show that the ratio of Bcl-2/Bax protein was decreased in ME- but not MI-treated cells (Fig. 2B). Furthermore, cleavage of the caspase 9 protein was also observed in ME-treated cells, represented here as the appearance of p35 and p17 fragments by Western blotting; the release of cyt c from mitochondria to the cytoplasm was observed under ME treatment by Western blotting, an indicative of mitochondrial dysfunction induced by ME (Fig. 2C). Neither caspase 6 nor 8 protein cleavage was observed in ME-treated HL-60 cells, represented here as no decrease in the pro-form of both proteins. Results of the caspase 3 activity assay using Ac-DEVD-pNA as a colorimetric substrate showed that ME significantly induced caspase 3 enzyme activity (Fig. 3C). As the same part of experiment, activation of caspase 9 but not caspases 1, 6 or 8 enzyme activity was identified in ME-treated HL-60 cells by enzyme activity assay using respective specific colorimetric substrates. These data indicate that activation of caspases 3 and 9 but not others was involved in ME-induced apoptosis in human HL-60 leukemia cells.

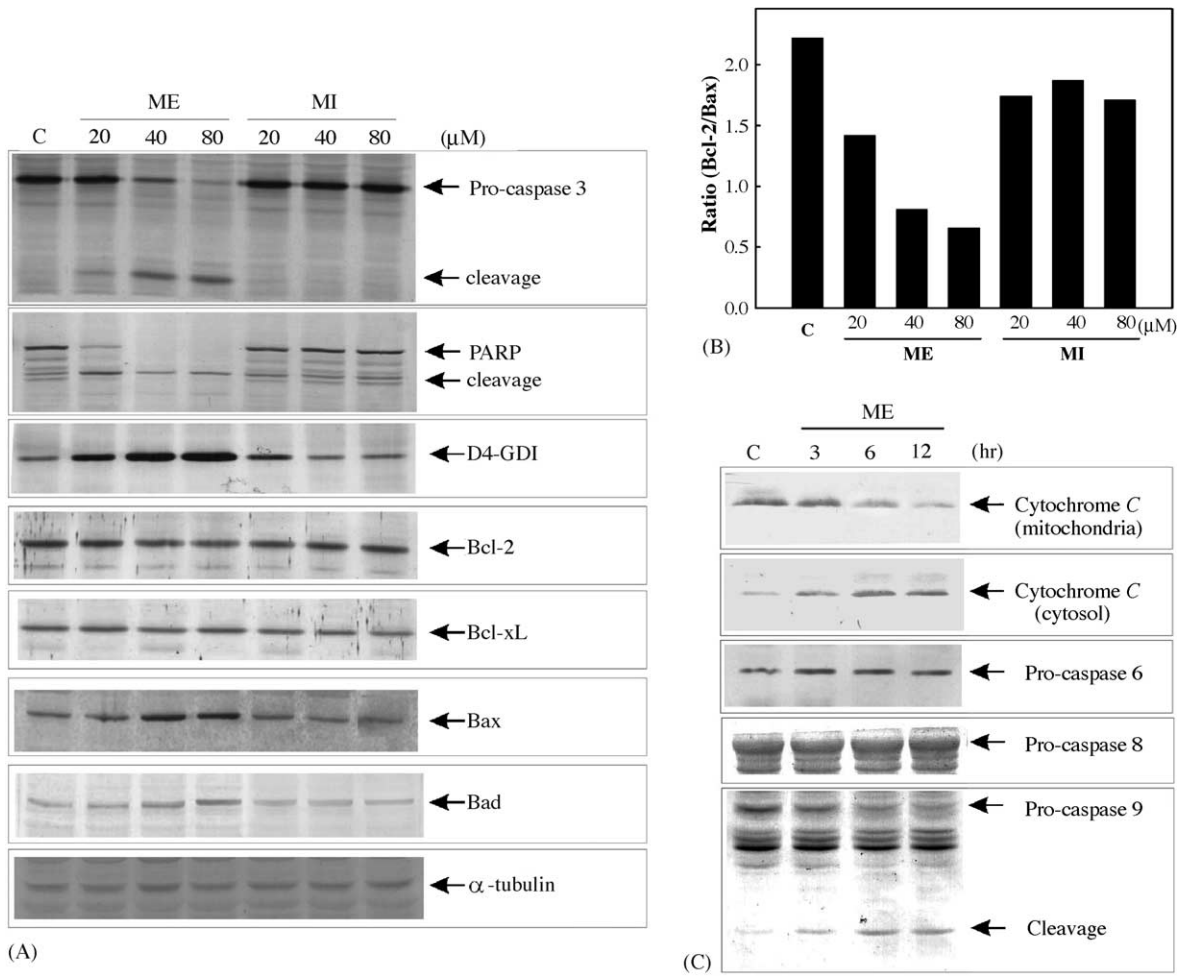

Fig. 2. Involvement of cytochrome c release from mitochondria to the cytosol, caspases 3 and 9 activation, PARP and D4-GDI protein cleavage, and alternative Bcl-2 family protein expressions in ME- but not MI-treated HL-60 cells. (A) HL-60 cells were treated with different concentrations of the indicated compounds for 12 h. Expressions of PARP, D4-GDI, caspase 3, Bcl-2 family proteins including Bcl-2, Bcl-XL, Bax, Bad, and an internal control α-tubulin protein were analyzed by Western blotting as described in Section 2. (B) The mean of the Bcl-2/Bax ratio was measured by densitometric quantification of data from three independent experiments. (C) Activation of caspase 6, 8, and 9 protein and release of cytochrome c from mitochondria to the cytosol were detected in myricetin-treated cells. Cells were treated with ME (80 μM) for 3, 6, and 12 h, and expression of the indicated protein was detected by Western blotting using specific antibodies.

3.3. Activation of caspase 9, located upstream of caspase 3 activation, is an essential event for ME-induced apoptosis

To further identify if activation of caspases 3 and 9 enzyme activities is an essential event for the apoptosis induced by ME, several specific peptidyl inhibitors of caspases were used in this study. As illustrated in Fig. 3A and B, addition of a caspase 3-like protease inhibitor (Ac-DEVD-FMK), a caspase 9-like protease inhibitor (Ac-LEHD-FMK), and a pan caspase inhibitor (Ac-VAD-FMK) significantly protected HL-60 cells from ME-induced DNA fragmentation and cytotoxicity. However, the caspase 1 inhibitor, Ac-YVAD-FMK, the caspase 6 inhibitor, Ac-VEID-FMK, and the caspase 8 inhibitor, Ac-IETD-FMK, showed no effect on cells under ME treatment. Additionally, adding the pan caspase inhibitor, Ac-VAD-FMK, and the caspase 9 inhibitor, Ac-LEHD-FMK, reduced caspase 3 enzyme activity and protein procession induced by ME (Fig. 3D). These data demonstrate that activation of caspase 3- and 9-like activity is an essential event for ME-induced apoptosis, and that caspase 9 activation is located upstream of caspase 3 activation.

3.4. ME-induced apoptosis is independent of ROS production

We investigated if ROS play an important role in ME-induced apoptosis. Results of Fig. 4A and B show that ME and MI alone did not affect the endogenous peroxide level in HL-60 cells. Interestingly, in the presence of H_2O_2, ME and MI significantly reduced H_2O_2-induced intracellular peroxide production by the DCHF-DA assay. Results of the anti-DPPH radical assay show that both ME and MI effectively decreased production of the DPPH radical activity, and the IC_{50} values for ME and MI were 8.13

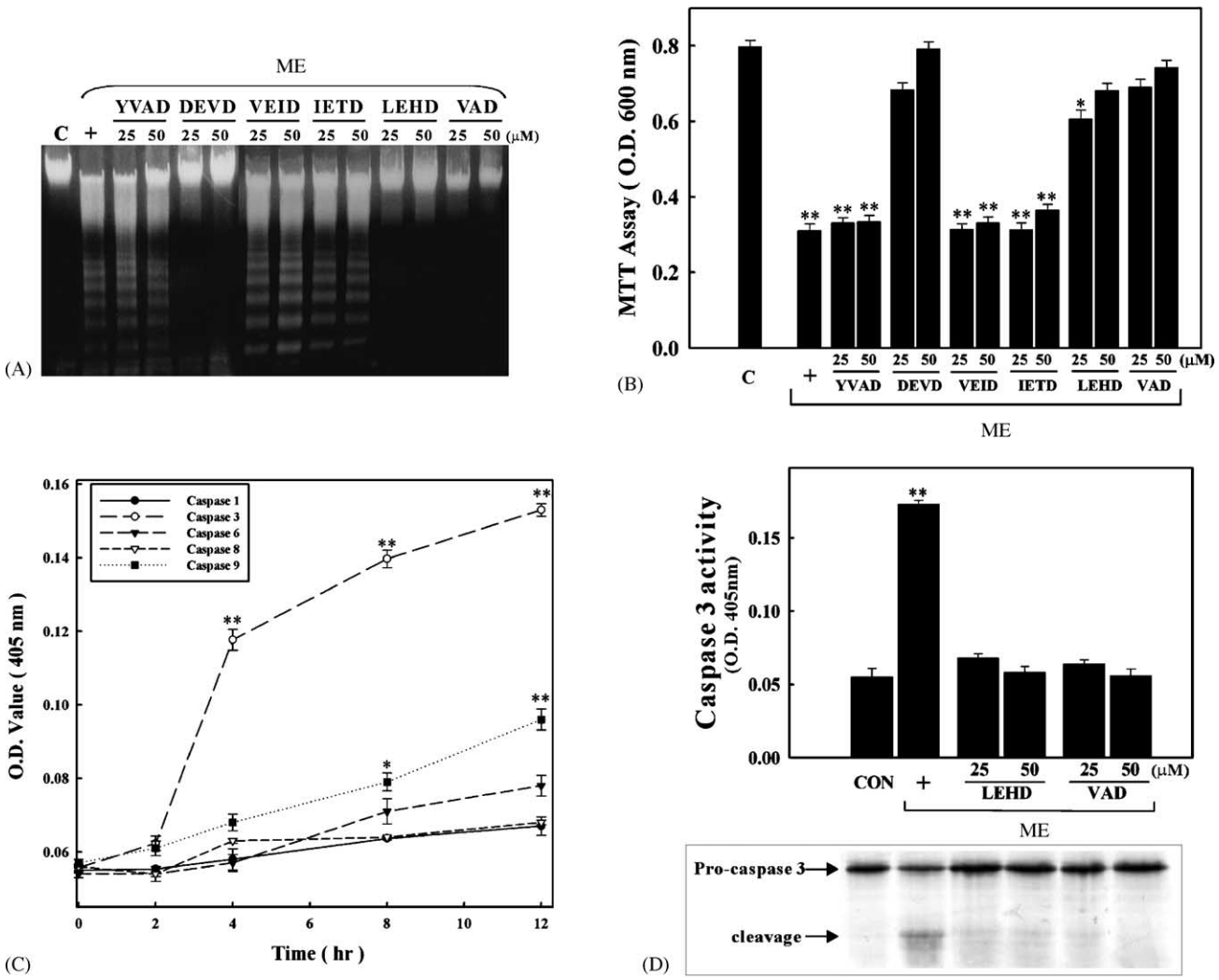

Fig. 3. Activation of caspases 3 and 9 but not caspases 1, 6, or 8 enzymes is involved in ME-induced apoptosis in HL-60 cells. (A) Differential protective effect of indicated caspase inhibitors on ME-induced apoptosis. Cells were treated with different doses (25 and 50 μM) of Ac-YVAD-FMK, Ac-DEVD-FMK, Ac-VEID-FMK, Ac-IETD-FMK, Ac-LEHD-FMK, or Ac-VAD-FMK for 3 h followed by ME (80 μM) for a further 12 h. The DNA fragmentation analysis was performed using 1.8% agarose electrophoresis. (B) Cell viability under the conditions described in (A) was examined by the MTT assay. (C) Elevation of caspases 3 and 9 but not 1, 6, or 8 enzyme activities in ME-treated HL-60 cells. Cells were treated with ME (80 μM) for different time points, and the indicated enzyme activities of caspases 1, 3, 6, 8, and 9 were detected using specific colorimetric substrates as described in Section 2. Each value is presented as the mean ± S.E. of three independent experiments. (*) $p < 0.05$ and (**) $p < 0.01$ significantly different from the control as analyzed by Student's *t*-test. (D) Activation of caspase 9 located upstream of caspase 3 activation in ME-treated HL-60 cells. Cells were pretreated with different doses (25 and 50 μM) of Ac-LEHD-FMK (a caspase 9 inhibitor) or Ac-VAD-FMK (a pan inhibitor) for 3 h followed by ME (80 μM) for a further 12 h. Enzyme activities of caspase 3-like proteases were analyzed (upper panel), and caspase 3 protein procession was detected by Western blots (lower panel).

and 7.18 μM, respectively (Fig. 4C). Furthermore, we used the plasmid digestion method induced by the Fenton reaction using H_2O_2 and Fe^{2+} as substrates to detect the effect of ME on ROS production in vitro. As elucidated in Fig. 4D, addition of ME reduced the damage to plasmids induced by the OH radical, represented here as a decrease in the intensity of the open-circle (OC) form and an increase in the intensity of the supercoiled form (SC) of the plasmid (Fig. 4D). Antioxidants such as *N*-acetylcysteine (NAC), catalase (CAT), superoxide dismutase (SOD), and tiron (TIR) protected HL-60 cells from H_2O_2-induced cell death (data not shown); however no protective effect against ME-induced apoptosis was observed by the DNA fragmentation and MTT assays (Fig. 4E and F). These data suggest that ME-induced apoptosis is independent of ROS production.

3.5. TPA significantly attenuates ME-induced apoptosis

12-*O*-Tetradecanoylphorbol 13-acetate has been recognized as a tumor promoter via PKC activation. In this study, HL-60 cells were pretreated with 100 ng/ml TPA for 1 h, and then ME-induced apoptosis was analyzed. As shown in Fig. 5A, TPA treatment induced the activity of alkaline phosphatase (AP) in HL-60 cells, an indicative of cellular differentiation. ME showed no effect on TPA-induced AP

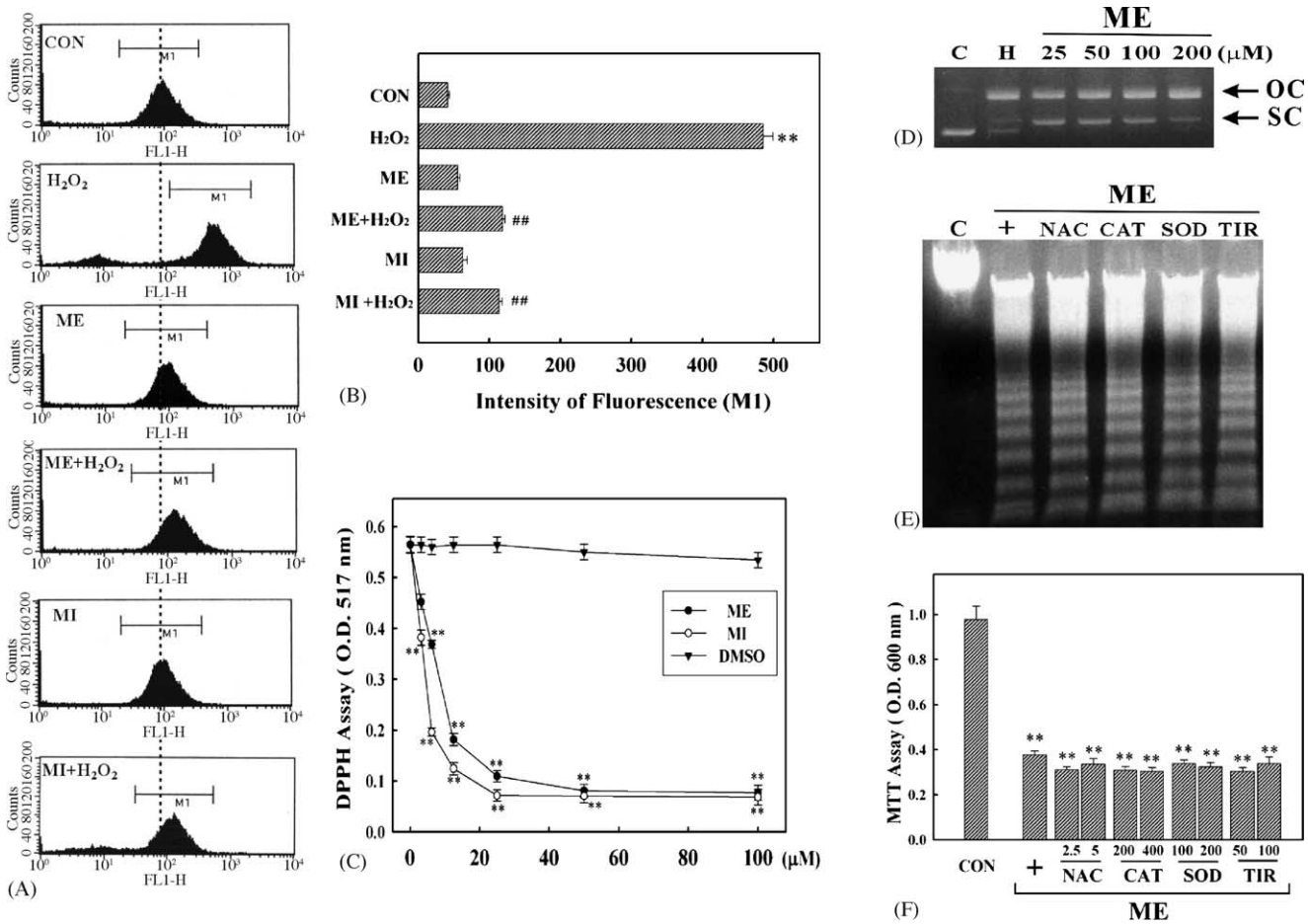

Fig. 4. ME-mediated apoptosis is independent of the production of reactive oxygen species (ROS). (A) HL-60 cells were, respectively, treated with 80 μM of ME or MI with or without 200 μM of H_2O_2 for 1 h, followed by DCHF-DA addition for an additional hour. The fluorescence intensity of cells was detected by flow cytometric analysis. A representative result of the flow cytometric analysis is presented here. (B) Quantification of the value of ME from three independent experiments is shown, and each value is expressed as the mean ± S.E. of three independent experiments. (**) $p < 0.01$ significantly different from the control as analyzed by Student's *t*-test. (C) In vitro anti-DPPH radical activities of ME and MI. Different concentrations (0, 20, 40, 60, and 80 μM) of ME or MI were added to 10 mM Tris–HCl (pH 7.9) containing 500 μM DPPH in methanol for 20 min. The value of OD517 was determined. Each value is expressed as the mean ± S.E. of three independent experiments. (D) ME inhibited OH radical DNA damage according to the plasmid digestion assay. The PBR322 plasmid was incubated with different doses of ME in the presence of an OH production system as described in Section 2. Changes in the conformation of the plasmid were analyzed by electrophoresis in 1% agarose. OC, open-circle form; SC, supercoiled form. (E) Antioxidants showed no protective effect against ME-induced DNA ladders in HL-60 cells. Cells were treated with different concentrations of NAC (20 mM), CAT (800 U/ml), SOD (800 U/ml), and TIR (20 μM) for 1 h followed by ME (80 μM) treatment for a further 12 h. The integrity of DNA was analyzed by electrophoresis as described previously. (F) As described in (E), the viability of cells under treatment with ME in the presence or absence of different doses of antioxidants was detected by the MTT assay. (*) $p < 0.05$ and (**) $p < 0.01$ significantly different from the control as analyzed by Student's *t*-test. NAC (2.5 and 5 mM), CAT (200 and 400 U/ml), SOD (100 and 200 μg/ml), TIR (50 and 100 μM).

activity. Interestingly, pretreatment of HL-60 cells with TPA protected cells from ME-induced cytotoxicity according to the MTT assay (Fig. 5B), and reductions in DNA laddering by electrophoresis (Fig. 5C) and in apoptotic bodies by microscopic observation induced by ME were observed (Fig. 5D). Additionally, results of flow cytometric analysis showed that TPA reduced the ratio of hypodiploid cells (sub-G1) induced by ME in HL-60 cells (Fig. 5E). The inhibitory percentage of TPA against ME-induced cytotoxicity and hypodiploid cells was about 80%. These results suggest that TPA possesses effective protective activity against ME-induced apoptosis.

3.6. Activation of PKC is involved in TPA prevention of ME-induced apoptosis in HL-60 cells

Activation of PKC is an early event in TPA-induced responses; therefore, we investigated if the protection of ME-induced apoptosis by TPA occurs through PKC activation. Results in Fig. 6A show that the addition of TPA induced activation of PKC, indicated here as translocation of PK Cα from the cytosol to the membrane by Western blotting. ME-induced apoptotic responses including caspase 3, caspase 9, PARP, and D4-GDI protein cleavage were effectively blocked by TPA addition. PKC inhibitors

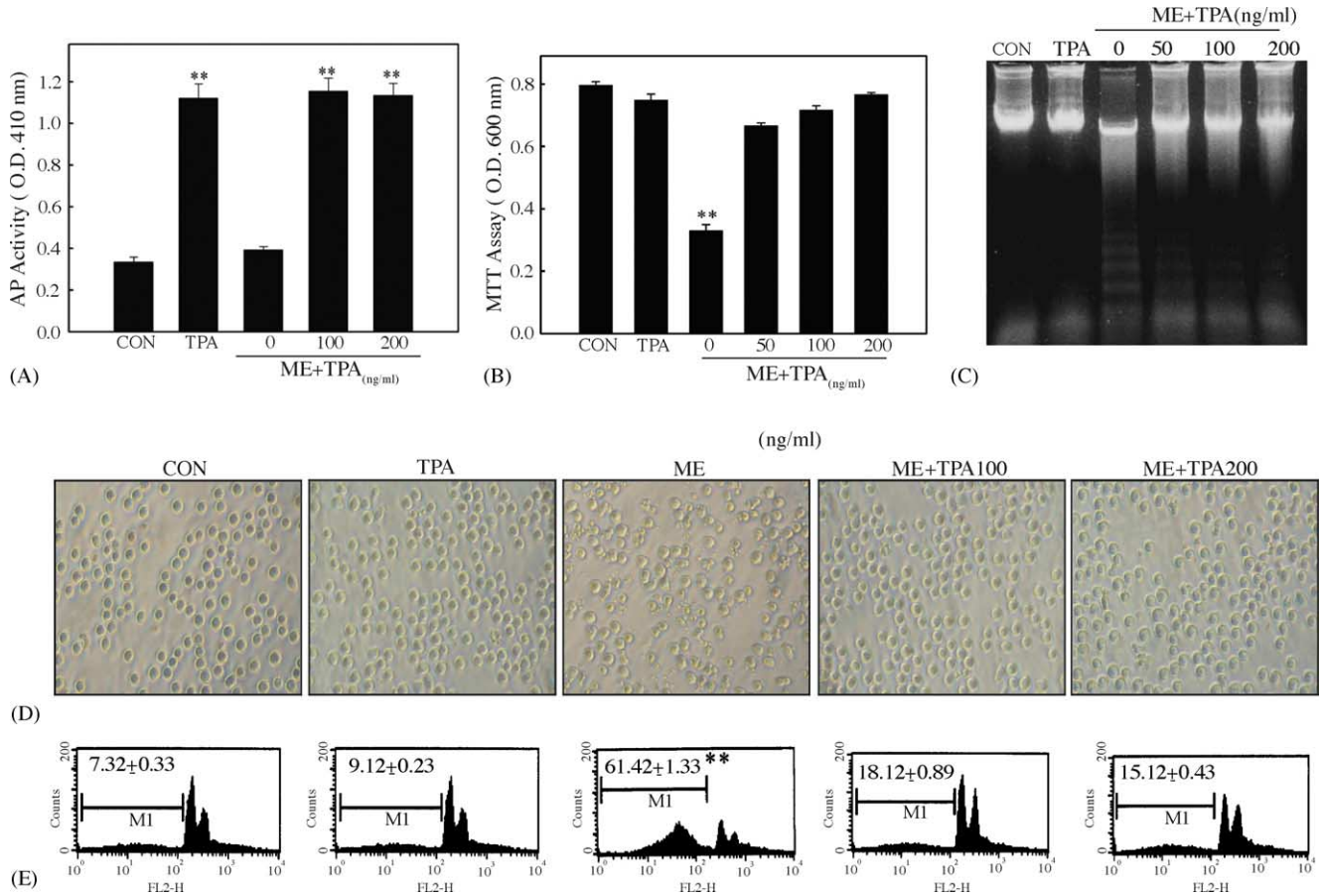

Fig. 5. TPA inhibited ME-induced apoptosis in HL-60 cells. (A) TPA treatment increased alkaline phosphatase (AP) activity in HL-60 cells. Cells were pretreated with or without TPA (100 or 200 ng/ml) for 1 h followed by ME treatment for a further 12 h. The alkaline phosphatase activity in HL-60 cells was performed using *p*-nitrophenol phosphate as an indicator, and OD405 was detected. (B) As described in (A), cells were pretreated with TPA (50, 100, and 200 ng/ml) for 1 h followed by ME (80 μM) treatment. The viability of cells under different treatments was detected by the MTT assay. (C) As described in (B), the integrity of DNA under different treatments was analyzed by electrophoresis in 1.8% agarose. (D) As described in (B), apoptotic bodies in ME-treated cells in the presence or absence of TPA (100 and 200 ng/ml) pretreatment were observed microscopically. (E) Hypodiploid cells (sub-G1) in ME-treated cells under the conditions were detected by flow cytometry. Each value is expressed as the mean ± S.E. of three independent experiments. (*) $p < 0.01$ significantly different from control as analyzed by Student's *t*-test.

such as staurosporine (ST), isoquinoline-5-sulfonic 2-methyl-1-piperazide (H7), and GF 109203X (GF) showed no cytotoxic or DNA laddering effect in cells without TPA and ME treatment. Interestingly, the inhibitory effect of TPA on ME-induced apoptosis was almost completely reversed by adding ST, H7, and GF, represented here as the reappearance of DNA ladders and a decrease in cell viability according to the MTT assay (Fig. 6B and C). Moreover, ME-induced cyt c release, a decrease in Bcl-2 protein, and an increase in Bax protein were inhibited by TPA, and these effects were significantly reversed by the addition of the PKC inhibitor, GF (Fig. 6D). These data suggest that activation of PKC is involved in TPA inhibition of ME-induced apoptosis.

3.7. Destruction of mitochondrial function is involved in ME-induced apoptosis

Previous data showed that release of cyt c from mitochondria to cytosol was detected in ME-treated HL-60 cells. Therefore, we further studied if ME-induced apoptosis occurs through destroying mitochondrial homeostasis. The mitochondrial membrane potential was detected by DiOC6(3) staining, and results described in Fig. 7A and B shows that ME treatment reduced the mitochondrial membrane potential which was prevented by TPA addition, represented here as a decrease in the fluorescence intensity by ME was prevented by TPA addition. Addition of PKC inhibitors including GF, H7, and ST reversed the protective effect of TPA on ME-induced a loss in mitochondiral membrane potential. In order to elucidate if mitochondria are an important target for the apoptotic induction by ME, EtBr-treated HL-60 cells were used in the present study. Previous studies indicated that a low dose of EtBr treatment might cause mitochondrial dysfunction [24–26]. Therefore, the sensitivity of HL-60- and EtBr-treated HL-60 cells to ME-induced apoptosis was analyzed. Results in Fig. 7C show that ME produced less of a DNA laddering effect in EtBr-treated cells, compared with parental cells. Similarly, a smaller cytotoxic effect of ME

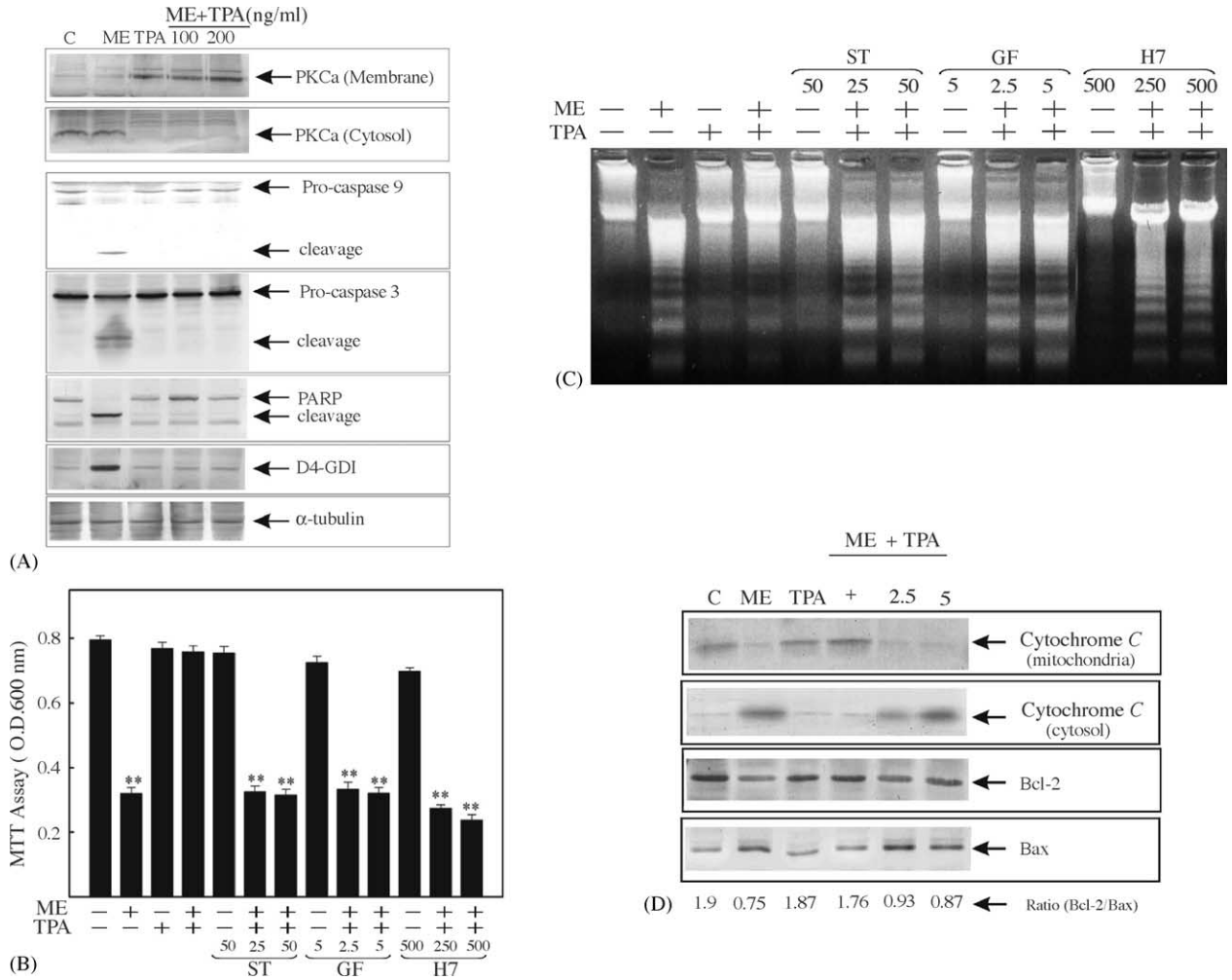

Fig. 6. Activation of PKC involved in TPA prevention of ME-induced apoptosis in HL-60 cells. (A) TPA induced PK Cα translocation from the cytosol to the membrane by inhibiting ME-induced apoptotic effects such as caspases 3 and 9 protein processing, and PARP and D4-GDI cleavage. Cells were pretreated with TPA (100 and 200 ng/ml) for 1 h followed by ME treatment for 1 h for PK Cα detection, and 12 h for detecting caspases 3 and 9 protein processing and PARP and D4-GDI cleavage by Western blotting. (B) The PKC inhibitors, ST (staurosporine; a broad-spectrum kinase inhibitor), H-7 (isoquinoline-5-sulfonic 2-methyl-1-piperazide; a PKA and PKC inhibitor), and GF (GF-109203X; a highly selective PKC inhibitor), reversed the protective effect of TPA against ME-induced apoptosis. Cells were pretreated with the indicated inhibitors with or without TPA for 1 h, followed by ME treatment (80 μM). The integrity of the DNA and cytotoxicity under different conditions were examined by (B) MTT assay and (C) DNA agarose gel electrophoresis. (**) $p < 0.01$ significantly different from the control as analyzed by Student's *t*-test. (D) TPA inhibited ME-induced cyt c translocation, a decrease in Bcl-2 protein, and an increase in Bax protein, which was blocked by the addition of the PKC inhibitor, GF, in HL-60 cells. Cells were incubated as described previously, and the expression of indicated proteins was detected by Western blotting.

was detected in EtBr-treated cells by the MTT assay (Fig. 7D). These data reinforced the notion that the disruption of mitochondrial homeostasis plays an important role in ME-induced apoptosis.

3.8. Hydroxyl groups at C3′, C4′, and C5′ are important for the cytotoxic effects of ME

In order to identify the important structural characteristics of ME, three additional structurally related compounds including flavone (Fla), myricetin trimethylether (ME-M), and galangin (Gal) were used in the present study. As shown in Fig. 8A, Fla possesses no OH group in its structure; ME-M is derived from ME in which three OH groups at C3′, C4′, and C5′ are replaced by OCH_3 groups in the B ring; and Gal is a compound without the three OH groups at C3′, C4′, and C5′ of ME. The cytotoxic potency of these compounds was ME > Gal > ME-M > Fla, and IC_{50} values of ME, Gal, ME-M, and Fla were 42.25, 102.3, >200, and >200 μM by MTT assay, respectively (Fig. 8B). Results of the DNA integrity assay show that ME exhibited the most-significant DNA laddering effect among these compounds in HL-60 cells (Fig. 8C). Gal, at the highest dose of 80 μM, showed a slight but significant DNA laddering effect in the study, however neither ME-M nor Fla exhibited an apoptotic effect at the tested doses in HL-60 cells. These data indicate that OH substitutions at C3′, C4′, C5′ are important for the apoptosis-inducing activity of ME.

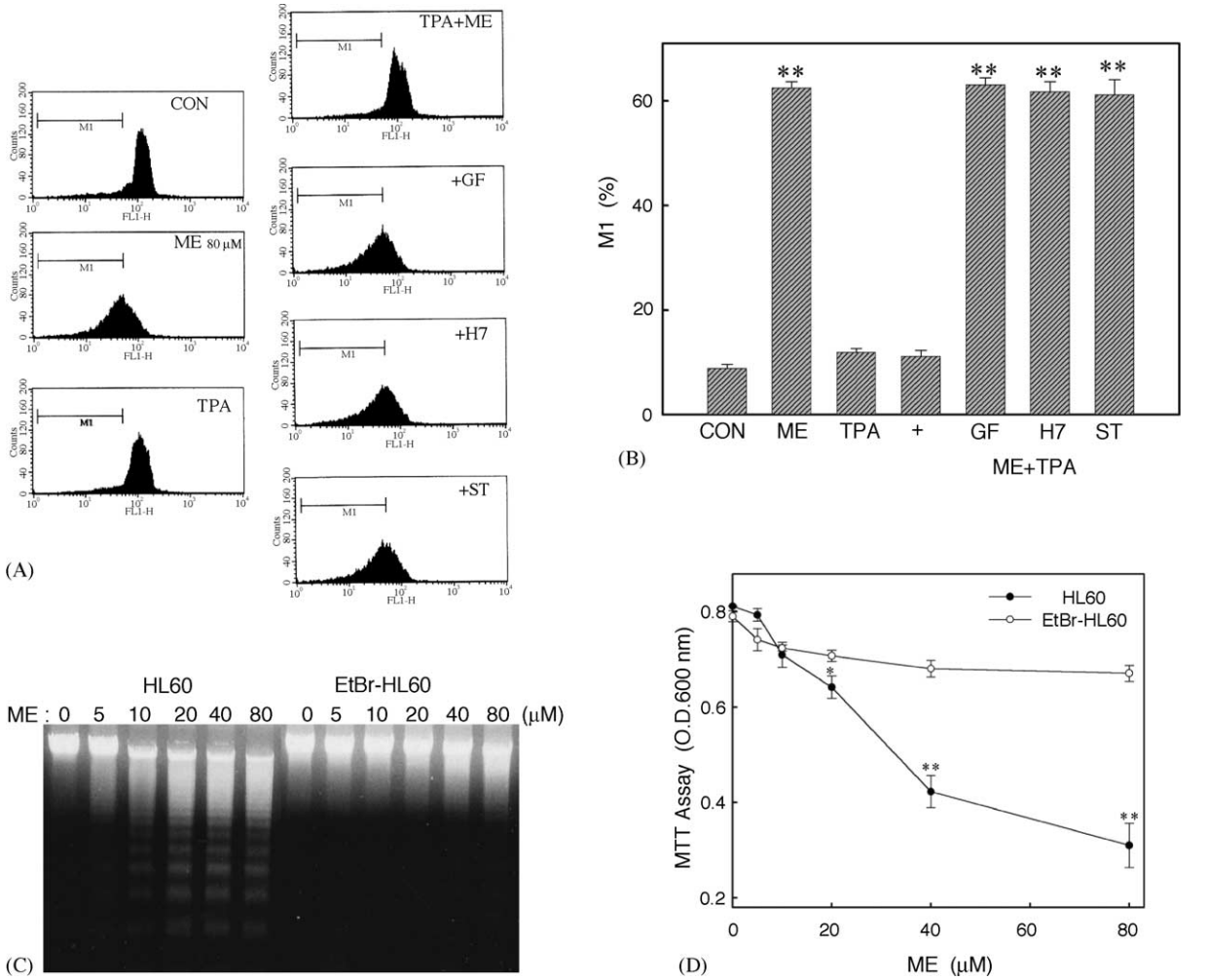

Fig. 7. Reduction of the mitochondrial membrane potential involved in ME-induced apoptosis. (A) ME reduced the mitochondrial membrane potential which was blocked by TPA. Cells were treated with TPA (100 ng/ml), TPA + GF (5 μM), TPA + H7 (500 nM), and TPA + ST (50 nM) for 1 h followed by ME (80 μM) treatment for a further 12 h. At the end of treatment, DiOC6(3) was added to the culture medium for a further 30 min. The fluorescence intensity of DiOC6(3) in cells was analyzed by flow cytometry. A representative of the data is presented here. (B) Quantification of M1 values from three independent experiments was performed, and results are expressed as the mean ± S.E. (C) Reduced DNA laddering effect of ME in EtBr-treated cells (mitochondria-depleted p^0 cells), compared with that in parental cells. Both parental cells and EtBr-treated cells were incubated with different doses (5, 10, 20, 40, and 80 μM) of ME for 12 h, and the integrity of DNA was analyzed. (D) As described in (C), the viability of cells was measured by the MTT assay. Each value is expressed as the mean ± S.E. of three independent experiments. (*) $p < 0.01$ significantly different from the control as analyzed by Student's *t*-test.

3.9. Specific apoptotic effects of ME occur in leukemia cells but not in primary human normal polymorphonuclear (PMN) cells or murine peritoneal macrophages (PMs)

Previous data demonstrated the apoptotic mechanism of ME in HL-60 cells; however, the apoptotic specificity of ME between leukemia cells and normal blood cells is still undefined. Therefore, an additional leukemia cell line of Jurkat cells and two normal blood cell lines derived from healthy human and murine blood including primary human PMN and murine peritoneal macrophages PM cells were used in the study. Results of the MTT assay showed that ME dose-dependently reduced the viability of Jurkat cells, but not that of PMN and PM cells (Fig. 9B). Induction of DNA laddering by ME was observed in Jurkat but not in PMN or PM cells (Fig. 9A). Similarly, induction of caspase 3 protein procession and PARP and D4-GDI cleavage was exhibited in ME-treated Jurkat but not in PMN or PM cells (Fig. 9C and data not shown). These data suggest specific apoptotic activity of ME in leukemia cells.

4. Discussion

Results of the present study show that apoptosis induced by ME occurred in a mitochondria-dependent, ROS-independent manner. Sequential activation of caspases 9 and 3 but not other caspases was involved in ME-induced apoptosis. Activation of PKC by TPA treatment protected cells from ME-induced apoptosis via maintaining mitochondrial homeostasis and inhibiting caspases 3 and 9 activation.

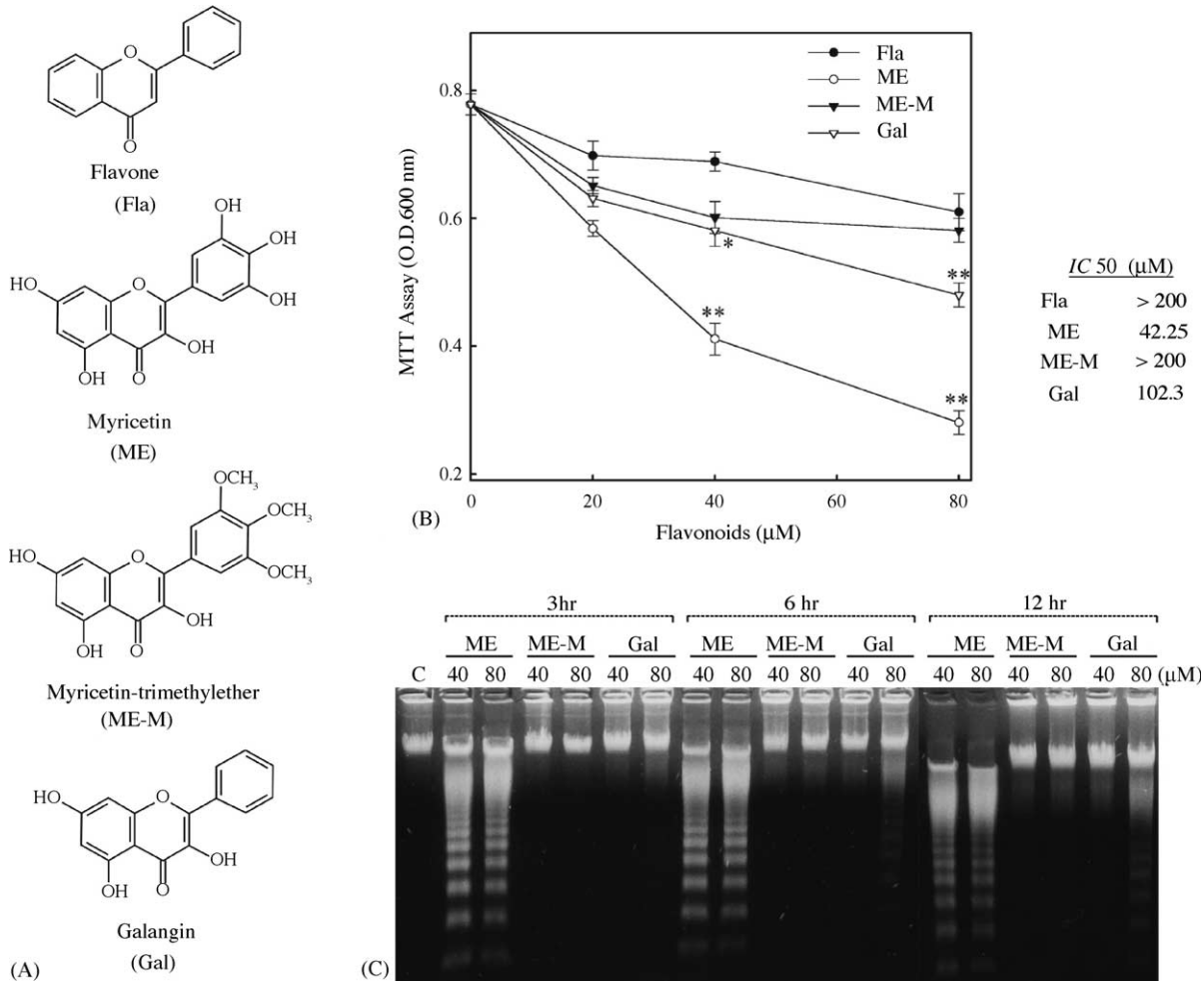

Fig. 8. Hydroxyl (OH) groups at C3′, C4′, and C5′ are important for the apoptosis-inducing activity of ME in HL-60 cells. (A) Structurally related compounds including flavone (Fla), myricetin, myricetin-trimethylether (ME-M), and galangin (Gal) were used in the study. (B) Different cytotoxicities in Fla-, ME-, ME–M-, and Gal-treated HL-60 cells were identified. Cells were treated with (20, 40, and 80 μM) of the indicated compounds for 12 h, the viability of cells was examined by the MTT assay as described previously, and IC_{50} values were measured. (C) Differential DNA laddering effect of the indicated compounds in HL-60 cells. Cells were treated with different doses (40 and 80 μM) of the indicated compounds for different time points, and DNA ladders were examined by agarose electrophoresis as described previously.

This suggests that abrogating mitochondrial function is important for apoptosis induction in leukemia cells, which might be independent of ROS production.

Mitochondria play essential roles in apoptosis through the redistribution of intermembranous mitochondrial proteins such as cyt c, and the mitochondrial membrane potential we considered causes opening of the permeability transition pore, which has been reported to be an irreversible step toward apoptosis [29,30]. A two-step process of cyt c release has been reported during apoptosis, and late cyt c release can be a consequence of caspase activation. Release of cyt c to the cytoplasm causes activation of caspase 9, located upstream of caspase 3 activation [31,32]. Caspase 3 is an executioner of apoptosis by cleavage of several essential cellular proteins such as PARP, D4-GDI, and Bcl-2 family proteins such Bcl-2. However, Chen et al. indicated that caspase 3 directly contributes to cyt c release in the absence of cytosolic factors [33,34]. Results of the present study show that activation of caspases 3 and 9 but not caspase 8, a caspase activated by the Fas ligand and which transduces apoptotic signals from the membrane, was identified in ME-induced apoptosis with a decrease in mitochondrial membrane potential and release of cyt c from mitochondria to the membrane. Addition of peptidyl inhibitors for caspases 3 and 9 but not for caspase 8 significantly attenuated ME-induced apoptosis, and caspase 9 inhibition by the specific inhibitor, Ac-LEHD-fmk, caused a decrease in caspase 3 enzyme activity and protein procession during ME treatment. These data reinforce the idea that apoptosis induced by ME occurs through mitochondria-dependent caspase activation.

The relationship between ROS and mitochondrial functions is not clear, although several previous studies provided both positive and negative evidence on this topic [35–37]. A number of apoptotic stimuli induce cyt c release and apoptosis via ROS production. However, ROS are able

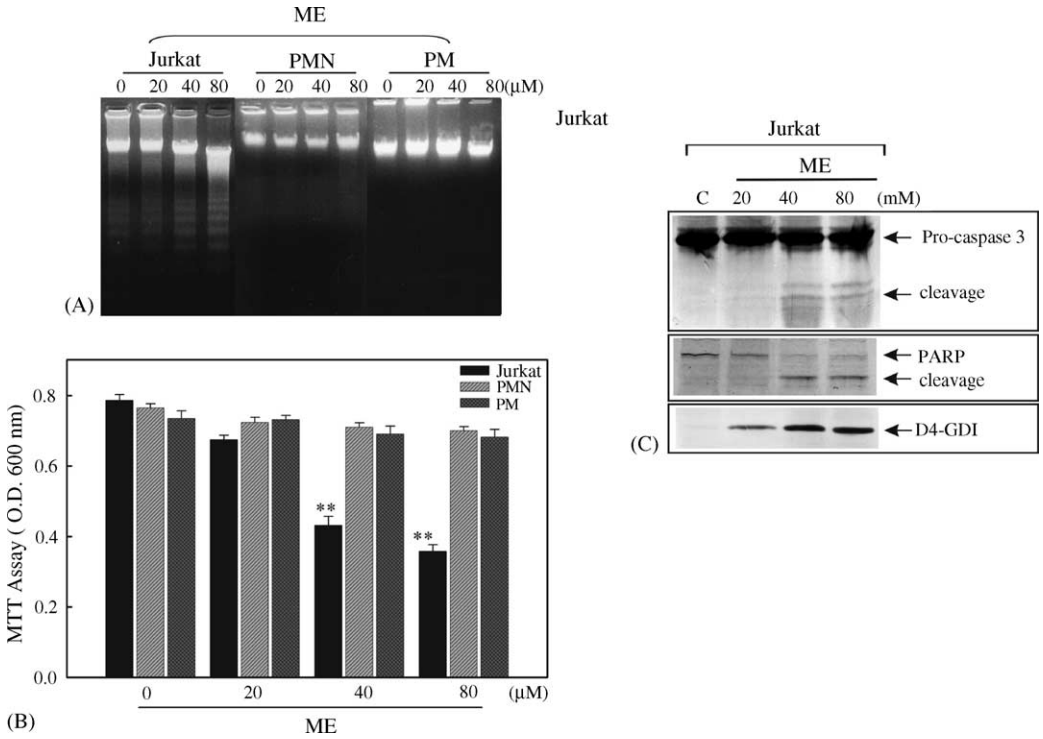

Fig. 9. Specificity of the apoptotic effect of ME in leukemia cells, but not in normal polymorphonuclear (PMN) cells or murine peritoneal macrophages (PMs). (A) Equal numbers of Jurkat cells, PMs, and PMN cells were treated with different concentrations (20, 40, and 80 μM) of ME for 12 h. Analysis of DNA fragmentation was performed by electrophoresis in 1.8% agarose. (B) The viability of cells under conditions as in (A) was examined by MTT assay. (C) Activation of caspase 3 processing and PARP and D4-GDI cleavage was identified in ME-treated Jurkat cells. Cleavage of PARP, D4-GDI, and caspase 3 proteins were detected by Western blotting as described previously. Each value is presented as the mean ± S.E. of three independent experiments. (**) $p < 0.01$ significantly different from control as analyzed by Student's *t*-test.

to play a role as mitogens to induce proliferation and protect cells from apoptosis induced by oxidative stresses [38,39]. These data suggest a double-sided function of ROS. In order to understand the complex functional relationships between the biochemical hallmarks for apoptosis including cyt c release, caspase activation, ROS production, and their regulation by Bcl-2 family proteins, analysis of the indicated genes' expressions and ROS productions by flow cytometry was performed in ME-treated cells. We found that apoptosis induced by ME is associated with the release of cyt c to the cytosol, caspase activation, and a decrease in Bcl-2 protein and an increase in Bax protein levels. However, no ROS production was detected in several ROS assay systems including the DPPH assay, plasmid digestion assay, antioxidant protection assay, and DCHF-DA assay under ME treatment. Therefore, mitochondria-dependent, ROS-independent apoptosis was suggested to occur in ME-treated cells. Previous studies including our own demonstrated that cells expressing high levels of ectopic Bcl-2 protein showed resistance to apoptosis induced by stimuli via preventing GSH depletion, cyt c release, and mitochondrial dysfunction [40–42]. In the present study, a decrease in the Bcl2/Bax protein ratio was found in ME-treated cells with loss of mitochondrial functions. This suggests that reduction of the Bcl-2 protein and induction of the Bax protein are involved in apoptosis induced by ME.

TPA is a tumor promoter and induces carcinogenesis in mouse skin models. Our previous studies identified several genes activated by TPA including PKC, ornithine decarboxylase (ODC), c-Jun, and PKC located upstream of ODC and c-Jun gene expression induced during TPA treatment [27]. Activation of PKC regulates several physiological roles including survival, proliferation, and apoptosis. PKC activation contributes to the resistance of cells to stimuli-induced apoptosis via activation of ERK1/2 [43]. Zhuang et al. indicated that PKC inhibits singlet oxygen-induced apoptosis by blocking activation of caspase-8 [44]. However, induction of apoptosis by TPA through activation of protein kinase C has also been identified, and inostamycin-induced apoptosis is mediated by PKC-regulated ceramide generation, leading to activation of a caspase cascade [45,46]. These data suggest that activation of PKC may both potentiate and decrease the generation of apoptosis. However, the effect of PKC activation on mitochondrial function during apoptosis is still unclear. The present results show that the addition of TPA protected cells from ME-induced apoptosis in accordance with inducing PKC translocation, reducing cyt c release to the cytoplasm, and maintaining the mitochondrial membrane potential (data not shown). The addition of the PKC inhibitor, GF 109203X, reversed the protective effect of TPA on ME-induced apoptosis with the reappearance of mitochondrial damage induced by ME. ME activation of downstream

caspases was also inhibited by pre-treatment of cells with TPA, and that was fully reversed by adding PKC inhibitors. We provide scientific evidence to indicate that TPA's protection against apoptosis occurs through PKC activation via maintaining mitochondrial functions in cells.

The locations of hydroxyl groups are important to the biological activities of flavonoids. Our previous studies demonstrated that rutinoside at C7 reduces both the apoptotic and anti-inflammatory activities of flavonoids, and OH groups at C4′ and C6 are important for the apoptosis-inducing activity of flavanone [20]. The present data support glycoside addition possibly attenuating the apoptosis-inducing activity of flavonoids because ME but not its glycoside MI exhibited a significant apoptotic effect in cells. Additionally, deletion of three OH groups at C3′, 4′, and 5′ of ME such as in galangin (Gal), replacement of three OH groups at C3′, 4′, and 5′ of ME by OCH_3 groups such as in ME-trimethylester (ME-M), or deletion of all six OH groups at C3, 5, 7, 3′, 4′, and 5, of ME such as in flavone (Fla) significantly reduced the apoptotic effect of ME, and the respective IC_{50} values of ME, Gal, ME-M, and Fla were 42.25, 102.3, >200, and >200 μM in HL-60 leukemia cells. These data strongly suggest that OH groups at C3′, 4′, and 5′ are important substitutions for the apoptosis-inducing activity of ME.

In conclusion, mitochondria-dependent apoptosis indicated by sequential events including reducing the mitochondrial membrane potential, inhibiting the Bcl-2/Bax protein ratio, releasing cyt c from mitochondria to the cytosol, and activating caspases 9 and 3 enzymes without ROS production was identified in the present study. Additionally, PKC activated by TPA prevented mitochondrial dysfunction induced by ME. ME shows no cytotoxicity in normal PMN and PM cells. A proposed mechanism of apoptosis induced by ME in leukemia cells was shown in Fig. 10.

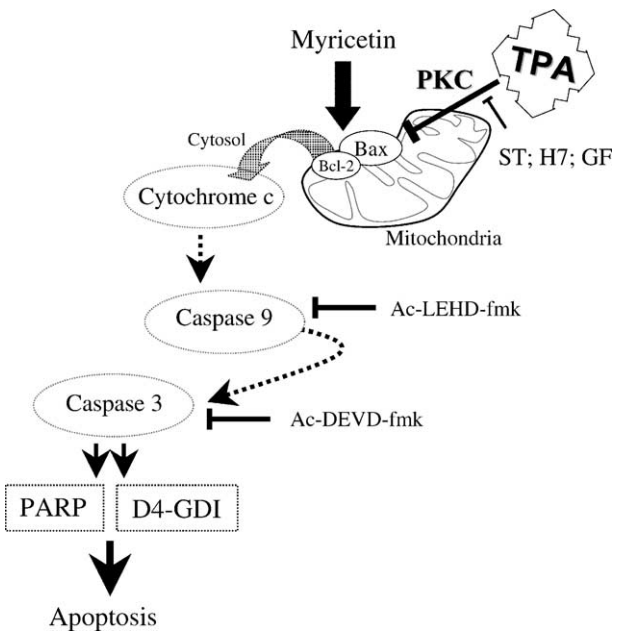

Fig. 10. A tentative model for ME-induced apoptosis in HL-60 cells as proposed in the present study. TPA, 12-*O*-tetradecanoylphorbol 13-acetate; PKC, protein kinase C; ST, staurosporine; H-7, isoquinoline-5-sulfonic 2-methyl-1-piperazide; GF, GF-109203X, and PARP, poly(ADP-ribose) polymerase.

Acknowledgement

This study was supported by grants (NSC93-2321-B-038-009, NSC92-2320-B-038-021, and NSC 92-2321-B-038-007) from the National Science Council, Taiwan.

References

[1] Seo YW, Shin JN, Ko KH, Cha JH, Park JY, Lee BR, et al. The molecular mechanism of Noxa-induced mitochondrial dysfunction in p53-mediated cell death. J Biol Chem 2003;278:48292–9.
[2] Katoh I, Tomimori Y, Ikawa Y, Kurata S. Dimerization and processing of procaspase-9 by redox stress in mitochondria. J Biol Chem 2004;279:15515–23.
[3] McDonnell MA, Wang D, Khan SM, Vander Heiden MG, Kelekar A. Caspase-9 is activated in a cytochrome c-independent manner early during TNFalpha-induced apoptosis in murine cells. Cell Death Diff 2003;10:1005–15.
[4] Burdick AD, Davis 2nd JW, Liu KJ, Hudson LG, Shi H, Monske ML, et al. Benzo(*a*)pyrene quinones increase cell proliferation, generate reactive oxygen species, and transactivate the epidermal growth factor receptor in breast epithelial cells. Cancer Res 2003;63:7825–33.
[5] Kreuzer J, Viedt C, Brandes RP, Seeger F, Rosenkranz AS, Sauer H, et al. Platelet-derived growth factor activates production of reactive oxygen species by NAD(P)H oxidase in smooth muscle cells through Gi1,2. FASEB J 2003;17:38–40.
[6] Perkins CL, Fang G, Kim CN, Bhalla KN. The role of Apaf-1, caspase-9, and bid proteins in etoposide- or paclitaxel-induced mitochondrial events during apoptosis. Cancer Res 2000;60:1645–53.
[7] Varbiro G, Veres B, Gallyas Jr F, Sumegi B. Direct effect of taxol on free radical formation and mitochondrial permeability transition. Free Radic Biol Med 2001;31:548–58.
[8] Slikker 3rd W, Desai VG, Duhart H, Feuers R, Imam SZ. Hypothermia enhances bcl-2 expression and protects against oxidative stress-induced cell death in Chinese hamster ovary cells. Free Radic Biol Med 2001;31:405–11.
[9] Steinman HM. The Bcl-2 oncoprotein functions as a pro-oxidant. J Biol Chem 1995;270:3487–90.
[10] Gabriel B, Sureau F, Casselyn M, Teissie J, Petit PX. Retroactive pathway involving mitochondria in electroloaded cytochrome c-induced apoptosis. Protective properties of Bcl-2 and Bcl-XL. Exp Cell Res 2003;289:195–210.
[11] Zhang XD, Borrow JM, Zhang XY, Nguyen T, Hersey P. Activation of ERK1/2 protects melanoma cells from TRAIL-induced apoptosis by inhibiting Smac/DIABLO release from mitochondria. Oncogene 2003;22:2869–81.
[12] Richard D, Lange S, Viergutz T, Kriehuber R, Weiss DG, Myrtill S. Influence of 50 Hz electromagnetic fields in combination with a tumour promoting phorbol ester on protein kinase C and cell cycle in human cells. Mol Cell Biochem 2002;232:133–41.
[13] Bezombes C, de Thonel A, Apostolou A, Louat T, Jaffrezou JP, Laurent G, et al. Overexpression of protein kinase Czeta confers protection against antileukemic drugs by inhibiting the redox-dependent sphingomyelinase activation. Mol Pharm 2002;62:1446–55.

[14] Harper N, Hughes MA, Farrow SN, Cohen GM, MacFarlane M. Protein kinase C modulates tumor necrosis factor-related apoptosis-inducing ligand-induced apoptosis by targeting the apical events of death receptor signaling. J Biol Chem 2003;278:44338–47.
[15] Tanaka Y, Gavrielides MV, Mitsuuchi Y, Fujii T, Kazanietz MG. Protein kinase C promotes apoptosis in LNCaP prostate cancer cells through activation of p38 MAPK and inhibition of the Akt survival pathway. J Biol Chem 2003;278:33753–62.
[16] Hah JO, Lee KA, Choi YJ, Kim WD, Park JW, Kwon TK. Inactive caspase 3 activates Akt in human leukemia cells susceptible or resistant to apoptosis induced by phorbol ester. Int J Oncol 2003;22:1111–6.
[17] Lin HY, Uan SH, Shen SC, Hsu FL, Chen YC. Inhibition of lipopolysaccharide-induced nitric oxide production by flavonoids in RAW264.7 macrophages involves heme oxygenase-1. Biochem Pharmacol 2003;66:1821–32.
[18] Shen SC, Ko CH, Tseng SW, Chen YC. Structurally related antitumor effects of flavanones in vitro and in vivo: involvement of caspase 3 activation, p21 gene expression and reactive oxygen species production. Toxicol Appl Pharmacol 2004;197:84–95.
[19] Chen YC, Shen SC, Lin HY. Rutinoside at C7 attenuates the apoptosis-inducing activity of flavonoids. Biochem Pharmacol 2003;66: 1139–50.
[20] Ko CH, Shen SC, Chen YC. Hydroxylation at c4′ or c6 is essential for apoptosis-inducing activity of flavanone through activation of the caspase 3 cascade and production of reactive oxygen species. Free Radic Biol Med 2004;36:897–910.
[21] Shen SC, Ko CH, Hsu KC, Chen YC. 3-OH flavone inhibition of epidermal growth factor-induced proliferation through blocking prostaglandin E_2 production. Int J Cancer 2004;108:502–10.
[22] Chen YC, Shen SC, Lee WR, Hsu FL, Lin HY, Ko CH, et al. Emodin induces apoptosis in human promyeloleukemic HL-60 cells accompanied by activation of caspase 3 cascade but independent of reactive oxygen species production. Biochem Pharmacol 2002;64: 1713–24.
[23] Field FJ, Born E, Murthy S, Mathur SN. Gene expression of sterol regulatory element-binding proteins in hamster small intestine. J Lipid Res 2001;42:1–8.
[24] Larm JA, Vaillant F, Linnane AW, Lawen A. Up-regulation of the plasma membrane oxidoreductase as a prerequisite for the viability of human Namalwa rho 0 cells. J Biol Chem 1994;269:30097–100.
[25] Armand R, Channon JY, Kintner J, White KA, Miselis KA, Perez RP, et al. The effects of ethidium bromide induced loss of mitochondrial DNA on mitochondrial phenotype and ultrastructure in a human leukemia T-cell line (MOLT-4 cells). Toxicol Appl Pharmacol 2004;196:68–79.
[26] Seidel-Rogol BL, Shadel GS. Modulation of mitochondrial transcription in response to mtDNA depletion and repletion in HeLa cells. Nucleic Acids Res 2002;30:1929–34.
[27] Ko CH, Shen SC, Lin HY, Hou WC, Lee WR, Yang LL, et al. Flavanones structure related inhibition on TPA-induced tumor promotion through suppression of extracellular signal-regulated protein kinases: involvement of prostaglandin E2 in anti-promotive process. J Cell Physiol 2002;193:93–102.
[28] Khan MA, Mustafa J, Musarrat J. Mechanism of DNA strand breakage induced by photosensitized tetracycline–Cu(II) complex. Mutat Res 2003;525:109–19.
[29] Akao M, O'Rourke B, Teshima Y, Seharaseyon J, Marban E. Mechanistically distinct steps in the mitochondrial death pathway triggered by oxidative stress in cardiac myocytes. Circ Res 2003;92:186–94.
[30] Papucci L, Schiavone N, Witort E, Donnini M, Lapucci A, Tempestini A, et al. Coenzyme q10 prevents apoptosis by inhibiting mitochondrial depolarization independently of its free radical scavenging property. J Biol Chem 2003;278(30):28220–8.
[31] Guo Y, Srinivasula SM, Druilhe A, Fernandes-Alnemri T, Alnemri ES. Caspase-2 induces apoptosis by releasing proapoptotic proteins from mitochondria. J Biol Chem 2002;277:13430–7.
[32] Qin JZ, Bacon P, Panella J, Sitailo LA, Denning MF, Nickoloff BJ. Low-dose UV-radiation sensitizes keratinocytes to TRAIL-induced apoptosis. J Cell Physiol 2004;200:155–66.
[33] Chen Q, Gong B, Almasan A. Distinct stages of cytochrome c release from mitochondria: evidence for a feedback amplification loop linking caspase activation to mitochondrial dysfunction in genotoxic stress induced apoptosis. Cell Death Diff 2000;7:227–33.
[34] Chen Q, Chai YC, Mazumder S, Jiang C, Macklis RM, Chisolm GM, et al. The late increase in intracellular free radical oxygen species during apoptosis is associated with cytochrome c release, caspase activation, and mitochondrial dysfunction. Cell Death Diff 2003; 3:323–34.
[35] O'Rourke TW, Doudican NA, Mackereth MD, Doetsch PW, Shadel GS. Mitochondrial dysfunction due to oxidative mitochondrial DNA damage is reduced through cooperative actions of diverse proteins. Mol Cell Biol 2002;22:4086–93.
[36] Frossi B, Tell G, Spessotto P, Colombatti A, Vitale G, Pucillo C. H_2O_2 induces translocation of APE/Ref-1 to mitochondria in the Raji B-cell line. J Cell Physiol 2002;193:180–6.
[37] Cai Z, Lin M, Wuchter C, Ruppert V, Dorken B, Ludwig WD, et al. Apoptotic response to homoharringtonine in human wt p53 leukemic cells is independent of reactive oxygen species generation and implicates Bax translocation, mitochondrial cytochrome c release and caspase activation. Leukemia 2001;15:567–74.
[38] Kops GJ, Dansen TB, Polderman PE, Saarloos I, Wirtz KW, Coffer PJ, et al. Forkhead transcription factor FOXO3a protects quiescent cells from oxidative stress. Nature 2002;419:316–21.
[39] Kim BY, Han MJ, Chung AS. Effects of reactive oxygen species on proliferation of Chinese hamster lung fibroblast (V79) cells. Free Radic Biol Med 2001;30:686–98.
[40] Rieber M, Rieber MS. *N*-Acetylcysteine enhances UV-mediated caspase-3 activation, fragmentation of E2F-4, and apoptosis in human C8161 melanoma: inhibition by ectopic Bcl-2 expression. Biochem Pharmacol 2003;65:1593–601.
[41] Slater EP, Stubig T, Lau QC, Achenbach TV, Rapp UR, Muller R. C-Raf controlled pathways in the protection of tumor cells from apoptosis. Int J Cancer 2003;104:425–32.
[42] Lee M, Hyun DH, Marshall KA, Ellerby LM, Bredesen DE, Jenner P, et al. Effect of overexpression of BCL-2 on cellular oxidative damage, nitric oxide production, antioxidant defenses, and the proteasome. Free Radic Biol Med 2001;31:1550–9.
[43] Fernandez C, Ramos AM, Sancho P, Amran D, de Blas E, Aller P. 12-*O*-Tetradecanoylphorbol-13-acetate may both potentiate and decrease the generation of apoptosis by the antileukemic agent arsenic trioxide in human promonocytic cells. Regulation by extracellular signal-regulated protein kinases and glutathione. J Biol Chem 2004;279: 3877–84.
[44] Zhuang S, Demirs JT, Kochevar IE. Protein kinase C inhibits singlet oxygen-induced apoptosis by decreasing caspase-8 activation. Oncogene 2001;20:6764–76.
[45] Sumitomo M, Shen R, Goldberg JS, Dai J, Navarro D, Nanus DM. Neutral endopeptidase promotes phorbol ester-induced apoptosis in prostate cancer cells by inhibiting neuropeptide-induced protein kinase C delta degradation. Cancer Res 2000;60:6590–6.
[46] Kawatani M, Simizu S, Osada H, Takada M, Arber N, Imoto M. Involvement of protein kinase C-regulated ceramide generation in inostamycin-induced apoptosis. Exp Cell Res 2000;259:389–97.